Decoding the coupled decision-making of epithelial-mesenchymal transition and metabolic reprogramming in cancer

Madeline Galbraith[1], Herbert Levine[2*], José Onuchic[1*], and Dongya Jia[3*]

Correspondence should be addressed to the following authors:

*Herbert Levine: h.levine@northeastern.edu

*José Onuchic: jonuchic@rice.edu

*Dongya Jia: dongya.jia@nih.gov

[1]Center for Theoretical Biological Physics, Rice University, Houston, TX, USA

[2]Center for Theoretical Biological Physics, Department of Physics, and Department of Bioengineering, Northeastern University, Boston, MA, USA

[3]Immunodynamics Group, Laboratory of Integrative Cancer Immunology, Center for Cancer Research, National Cancer Institute, Bethesda, MD, USA

Abstract

Cancer metastasis is an orchestration of multiple traits driven by different functional modules such as metabolism and epithelial-mesenchymal transition (EMT). Cancer cells can adjust their metabolism during metastasis, but the underlying mechanisms remain unclear. When leaving the primary tumor and entering blood circulation, cancer cells can increase their oxidative phosphorylation (OXPHOS) without compromising glycolysis, thus acquiring a hybrid metabolic phenotype (W/O) with a high metastatic potential. In many cases, EMT serves as the primary instigator of metastasis. Cancer cells undergoing EMT can acquire a hybrid epithelial/mesenchymal (E/M) phenotype, combining epithelial and mesenchymal features. To decipher how metabolism drives metastasis and vice versa, we couple the decision-making networks of metabolism and EMT to elucidate how crosstalk effects the stability of the E/M-W/O state. We show crosstalk can give rise to the E/M-W/O state, irrespective of individual E/M

or W/O availability. Additionally, to acquire an E/M-W/O state, the W/O state emerges first and is followed by the E/M state, suggesting metabolism may be a primary driver of EMT. In summary, our work emphasizes the mutual activation of the metabolism module and EMT module, and serves as an initiative towards understanding the entirety of cancer metastasis.

Introduction

Metastasis remains the leading cause of cancer-related deaths [1] and it is critical to understand the physiological properties of cells that migrate from the primary tumor and initiate metastatic lesions. Typically, these properties have been studied one at a time. For example, during the epithelial-mesenchymal transition (EMT) cells progressively lose epithelial (E) features such as cell-cell adhesion and apical-basal polarity, and acquire mesenchymal (M) features such as migration, invasion, and resistance to immune response [2]. The EMT has consistently been implicated in cells acquiring metastatic potential [3] and therapeutic resistance [4]. Recently, the bimodal picture of EMT has been superseded by a more complex scenario involving the hybrid epithelial/mesenchymal (E/M) phenotype which exhibits combined traits of epithelial (cell-cell adhesion) and mesenchymal (invasion) at the single-cell level. The existence of a hybrid E/M state has since been experimentally verified and associated with therapy resistance alongside poor survival rates [5–8]. Importantly, hybrid E/M cells migrate collectively and appear to be the most capable of initiating metastatic growth [8–13]. Fully understanding the behavior of the hybrid E/M phenotype is still an active area of research.

Metabolic reprogramming, another hallmark of cancer, enables cancer cells to adjust their metabolic activity for biomass and energy supply to survive in hostile environments [1,14]. Normal cells typically utilize oxidative phosphorylation (OXPHOS, O) under normoxic

conditions and glycolysis under hypoxic conditions. However, cancer cells often prefer glycolysis even when oxygen is available (i.e., the Warburg effect (W) or aerobic glycolysis) [15,16]. During metastasis, cancer cells adjust their metabolic phenotype to survive in varying environments, resulting in cells switching between different types of metabolism [17–19]. Metabolic reprogramming can enable cancer cells to combine different metabolic modes, such as acquisition of a hybrid W/O phenotype[20]. The W/O phenotype is associated with enhanced metabolic potentials, high metastatic potential [21,22], and actively uses both glycolysis and OXPHOS [23,24]. This suggests a tight connection between metabolic plasticity and cancer metastasis, specifically the hybrid W/O state with high metastatic potential.

As already mentioned, many studies of metastasis focused on either EMT or metabolism[10–13,17–19]. However, it has become increasingly clear extensive crosstalk exists between EMT and metabolism [22]. Recent studies show metabolic reprogramming can drive EMT and increase metastatic potential, or induction of EMT can drive metabolic reprogramming [25–29]. The underlying mechanisms that control how the metabolism functional module drives the EMT functional model, and vice versa, remain poorly understood, with several hypotheses as discussed below. Kang et. al. suggested cancer cells typically undergo metabolic reprogramming first and then trigger EMT [30]. This coupling, presumably, is a consequence of changes in the tumor microenvironment (TME) fostering metabolic reprogramming which drives EMT [28,29]. Another hypothesis is mutual activation between EMT and metabolic reprogramming contribute to flexible coupling of various EMT states with metabolic states. Possibly, the two hybrid phenotypes (E/M and W/O) become coupled under certain crosstalk, leading to greatly increased metastatic potential [22]. Evidence supporting this connection has recently been noticed in CTCs which exhibit enhanced OXPHOS with no compromise in glycolysis [31] and they may consist

mainly of hybrid E/M cells, especially at high levels of antioxidation regulator NRF2 [32]. Additionally, hybrid E/M-like breast cancer stem cells exhibit increased levels of OXPHOS and glycolysis [33,34]. While there have been preliminary indications of the coupling of EMT and metabolic states, a systematic analysis of the coupling between these states remains to be explored.

To decode the coupled decision-making of EMT and metabolism, we developed a mathematical model which couples the core gene regulatory circuit of EMT – μ_{34}/SNAIL/μ_{200}/ZEB [10] with that of metabolism – AMPK/HIF-1/ROS [20]. By analyzing the coupled circuit, we identified the μ_{34}/HIF-1/mtROS/μ_{200}/SNAIL axis as a key promoter of the coupled E/M-W/O state. Additionally, as we will show later, HIF-1 may play a more central role in metabolism driving EMT than AMPK. Strikingly, we found bidirectional crosstalk ensures parameter space regions exist for which only the E/M-W/O state is the only accessible state, and the biological significance of these parameters will depend on details of the microenvironment. Interestingly, even if the individual circuit cannot give rise to the hybrid phenotype (i.e., neither the E/M or W/O states are initially accessible), upon including crosstalk, the coupled E/M-W/O state emerges. Our results therefore suggest a highly aggressive plastic phenotype along both the EMT and metabolic axes (E/M-W/O) is a likely choice for a subset of cancer cells and, speculatively, may be critical for metastasis.

Model: Coupling the regulatory networks of EMT and metabolism

While the mechanisms of EMT and cancer metabolism have been investigated individually, the crosstalk between the two circuits and phenotypic correlations are still largely unknown. To decode the crosstalk between EMT and metabolism, we couple our previously

published regulatory networks of EMT [10] and metabolism [20] by including the mutual regulatory links between these two circuits; see Fig. 1A for the coupled network and Table S5 for details of the crosstalk. The crosstalk between the EMT and metabolism circuits can be direct (e.g., HIF-1 upregulating SNAIL) or indirect (e.g., μ_{34} upregulating mtROS), the latter arising because our formulation focuses only on a few core components and effective interactions between them can occur via intermediate reactants. We initially focus on the core networks and investigate the role of crosstalk on the coupling of EMT and metabolism states. Then we examine whether crosstalk contributes to the emergence of the hybrid states and the stability of the E/M-W/O state.

Previous investigations presented individual insight into the core EMT and metabolism networks. Exploration of the core EMT network by Lu and collaborators showed the μ_{200}/ZEB module was responsible for EMT tristability – epithelial (E, high μ_{200}/low ZEB), mesenchymal (M, low μ_{200}/low ZEB), and E/M (intermediate μ_{200}/intermediate ZEB) – whereas the μ_{34}/SNAIL module mainly acted as a noise buffer [10](see Fig. 1B, and section S2.1). In a separate line of investigation, a proposed regulatory circuit of metabolism AMPK/HIF-1/ROS, provided insight into cancer metabolism plasticity and switching between different metabolic phenotypes. Through this reduced circuit, Yu and collaborators show cancer cells can acquire at least three different metabolic phenotypes – OXPHOS (high AMPK/low HIF-1), Warburg (low AMPK/high HIF-1), and W/O (intermediate AMPK/HIF-1) [20] (see Fig. 1C).

To couple the regulatory circuits of EMT and metabolism, we did extensive literature search and identified the main bi-directional crosstalk between these two circuits (see Fig. 1A). Please refer to supplementary Table S5 for a detailed description of the included crosstalk. We utilize a framework consistent with the individual models of the EMT and metabolism network,

treating the coupled network as a transcription-translation chimeric circuit [10]. The transcriptional regulation is mathematically represented as a shifted Hill function [35], where the fold change (λ) represents the magnitude of the activation (λ >1) or inhibition (0=<λ <1). For readability of the figures, we define the parameter Λ=1-λ such that maximal inhibition occurs when Λ=1 (λ=0) and no inhibition when Λ=0 (λ=1). We also consider the binding/unbinding dynamics (e.g., mir200 silencing HIF-1), where the functions Y_μ, Y_m, and L represent the active miRNA degradation rate, active mRNA degradation rate, and translation rate (details in SI section 1.1, Fig. S1).

The new model we propose here is built by including these crosstalk links to couple the circuits of EMT and metabolism (see SI Section 1 for the full equations, parameters and brief explanation). We started with parameters such that both the EMT and metabolic networks are tristable. When the crosstalk is inactive, at maximum nine possible combinations of the EMT and metabolic phenotypes occur: E-W, E-O, E-W/O, M-W, M-O, M-W/O, E/M-W, E/M-O, and E/M-W/O (Fig. 1D, details of numerical integration and analysis are given in section S2). By activating the regulatory links, we can identify how the crosstalk affects the coupling between EMT states and metabolism states.

First, we must develop a classification of these coupled states. While the W state is characterized by high HIF-1/low AMPK and the E state by high μ_{200}/low ZEB expression, including the crosstalk will quantitatively alter the expression profiles for the various steady states. Therefore, the use of fixed thresholds to determine the state of the cell is no longer appropriate. Instead, we use a distance metric normalized by the expression of the decoupled network to classify the generated expression profiles as indicative of one of the nine coupled states (see Section S2.3 for details). With our baseline decoupled network parameters, we show

the hybrid states (W/O and E/M) are most populous followed by the W and M states, with the O and E states being least populated (Fig. S2-S4, note the frequency of these states depends on the model parameters).

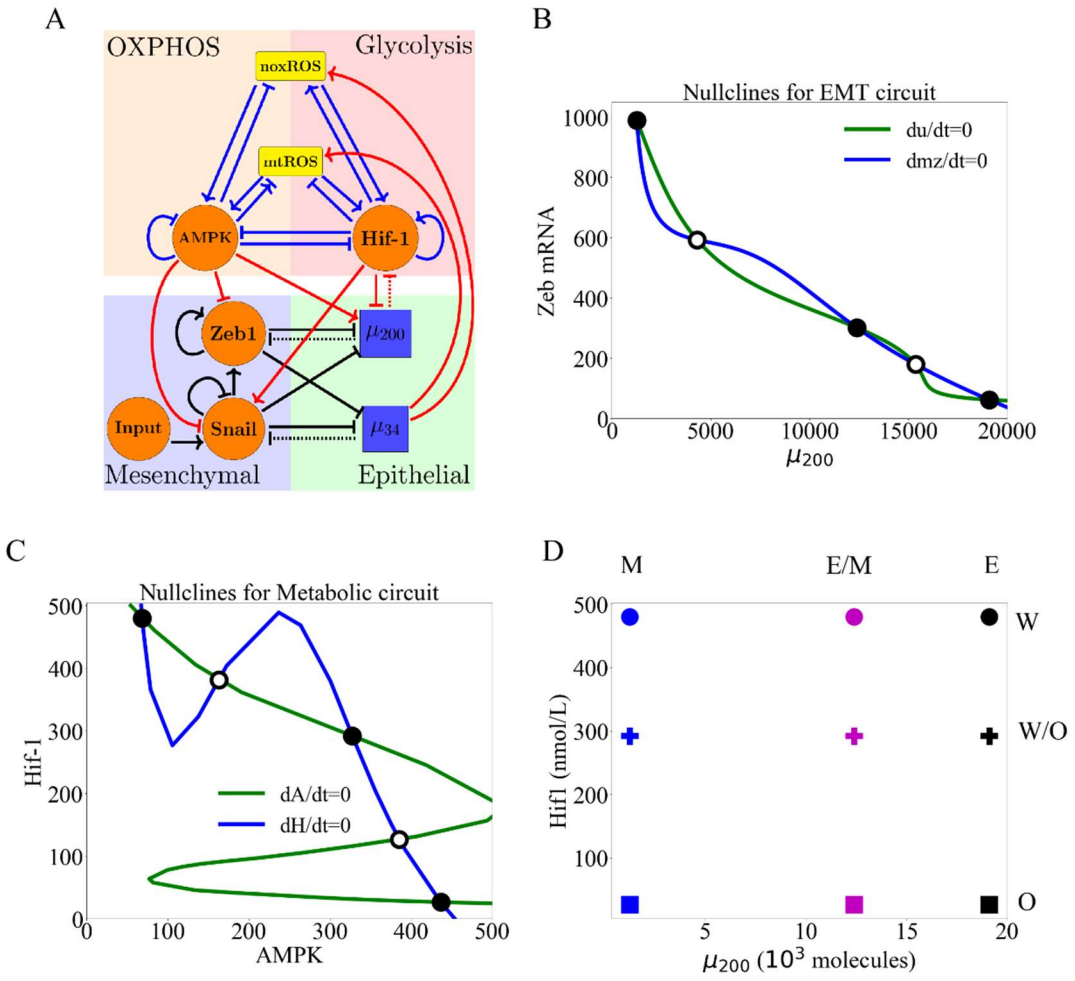

Figure 1. **The coupled EMT/MR circuit results in nine possible steady states. (A)** The network showing the core EMT module (bottom), the core metabolic module (top), and the crosstalk noted in red. The dashed lines denote miRNA-based regulation. Regulatory links ending in bars represent inhibition while arrows represent activation. **(B)** The nullclines of the EMT network. The system is tristable with states E (high μ_{200}/low Zeb) , M (low μ_{200}/high ZEB), and E/M (intermediate μ_{200}/ZEB). **(C)** The nullclines of the metabolic network. The system is tristable with stable states O (high AMPK/low HIF-1), W (low AMPK/high HIF-1), and W/O (intermediate AMPK/HIF-1). **(D)** The nine possible states when all crosstalks are inactive. The blue, purple, and black markers represent the EMT states. The circle, cross, and square represent the metabolism states (e.g., the coupled E/M-W/O state is represented as a purple cross).

Results

Individual crosstalk can push the downstream circuit towards a single state: Let us start by making just one crosstalk active, e.g., caused by an EMT-related microRNA. Now, in our model there is an unaffected upstream subnetwork (EMT, from where the link originates) and a regulated downstream one. (Note the model ignores any possible dilution of the microRNA due to its action on ROS; see below).

When noxROS is upregulated by μ_{34} (Fig. 2A), as there is no feedback to the EMT network, the occupancy of the E, E/M, and M states are unchanged. As the level of noxROS increases, the W-associated states are lost; first the E-W state, then the E/M-W, and finally the M-W state (Fig. 2B, section S2.4). Additionally, as noxROS increases, the W/O-associated states are stabilized and little change occurs for O-associated states (Fig. 2C). Upon analyzing the coupled states, if noxROS increases then the E/M state becomes more likely to be associated with the W/O state (Fig. 2D). Additionally, the W state is most associated with the M state which is expected since the M state has the lowest μ_{34} level, resulting in a smaller increase of noxROS compared with other EMT states (Fig. 2E).

Similar changes have been observed via μ_{34} upregulating mtROS. Consistent with upregulating noxROS, the E-W and E/M-W states are suppressed first and the E/M-W/O state is stabilized (Fig. S5). Additionally, upregulating mtROS exhibited a greater increase in the E/M-W/O state than upregulating noxROS. Further, activation of mtROS stabilizes the W/O state but reduces occupancy of the O state and W state. Together, these results suggest mtROS and noxROS may be critical factors in regulating the coupling of two hybrid states (E/M-W/O).

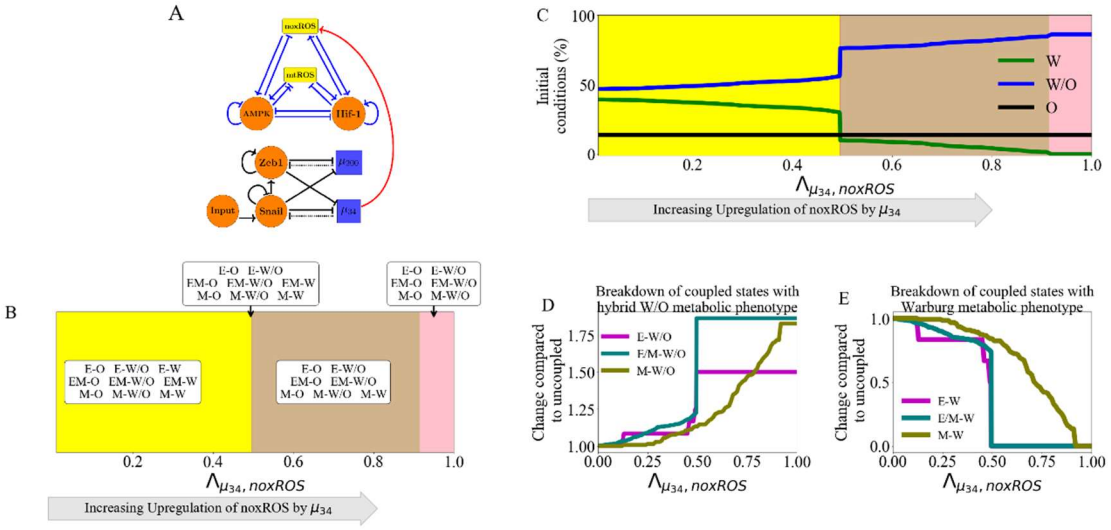

Figure 2. noxROS upregulated by μ_{34} stabilizes the W/O state and enhances the E/M-W/O coupled state. (A) A diagram of the core EMT (bottom) and metabolic (top) circuits connected by the crosstalk μ_{34} upregulating noxROS (red link). The EMT network is unchanged, as there is no feedback. **(B)** As μ_{34} upregulates noxROS, 4 distinct phases occur; all nine couple states followed by loss of the E-W, E/M-W, and M-W states (yellow, red, tan, and pink regions, respectively). **(C)** The lines represent the number of initial conditions leading to the W (green) , O (black), or W/O (blue) states as noxROS increases. (Background colors correspond to the phase colors of (B).) **(D)** The frequency of the W/O-associated states (i.e., E-W/O, M-W/O, and E/M-W/O) compared to the inactive system ($\lambda_{\mu_{34},noxROS} = 1$). All W/O-associated states are promoted, with the E/M-W/O state being greatly increased once $\lambda_{\mu_{34},noxROS} = 0.5$. **(E)** Same as (D) but for W-associated states. The W-associated states are suppressed with the M-W state lasting longest.

Regulation of HIF-1 affects both subcircuits: While the μ_{34} links only affect the downstream network, the miRNA regulation of HIF-1 by μ_{200} can affect both networks. This arises in our model because μ_{200} mediates the transcription and translation of HIF-1 mRNA, and as a result, μ_{200} can be recycled or degraded. Therefore, while the downstream metabolic network is modulated, the upstream EMT network is also affected via change of μ_{200}. We have defined a silencing function $P_H(\mu)$ to simulate the above-mentioned effect of μ_{200} on HIF-1 (details of function in section S2.5). Note as silencing increases, the restriction of the EMT states occur

immediately; close to $P_H(\mu) = 0$, the only EMT state allowed is M while all the metabolic phenotypes are allowed. As μ_{200} silences HIF-1, the W/O and W states are suppressed sequentially, and the O state is promoted. Additionally, as HIF-1 levels decrease, less degradation of μ_{200} (caused by binding to HIF-1 RNA) occurs, resulting in gradual disappearance of the M state. Thus, when HIF-1 mRNA is fully silenced, only the E-O and E/M-O states remain (Fig. S6). Since the E/M state does not reappear until after the metabolic system has fully transitioned to O, the E/M-W/O state is not observed for any value of μ_{200} silencing HIF-1 mRNA. These results suggest μ_{200} overexpression could promote the O-associated states (E-O and E/M-O) and destabilize the coupled E/M-W/O state.

Inclusion of multiple miRNAs of the EMT network can stabilize the W/O metabolic phenotype: We next wish to determine how including links emanating from both μ_{200} and μ_{34} can synergistically drive metabolic reprogramming and promote the coupled E/M-W/O state. While upregulating ROS causes an increase in the E/M-W/O state, we showed μ_{200} silencing HIF-1 suppresses the E/M-W/O state; therefore, we expect some suppression of the E/M-W/O state when including both μ_{200} and μ_{34} crosstalks. Interestingly, the E/M-W/O state can be fully suppressed when decreasing HIF-1 and upregulating noxROS, but only partially suppressed when decreasing HIF-1 and upregulating mtROS (Fig. S7). These results suggest the type of ROS present has different effects on the existence of the E/M-W/O state.

The E/M-W/O state is stabilized if mtROS is upregulated, but upregulating noxROS has minimal effect on the E/M-W/O state. Strikingly, when all miRNA crosstalks are active (μ_{200} silencing HIF-1, and μ_{34} upregulating noxROS and mtROS, Fig. 3A) the E/M-W/O state can be suppressed even if the W/O state is present (Fig. 3B). Further, the E/M-W/O state is present for all values of noxROS but is only present at increased levels of mtROS (Fig. 3B-C and S8).

Additionally, at high levels of mtROS, the E/M and W/O states are likely to be associated, suggesting upregulating mtROS can stabilize the E/M-W/O state (Fig. 3C). Depending on the initial conditions, the E/M-W/O state is accessible if HIF-1 is partially silenced and at high levels of noxROS and mtROS (Fig. 3D). This suggests there is a synergistic effect between the crosstalks, resulting in an increased parameter space enabling the E/M-W/O state than expected based on the individual crosstalks. Further, the difference in the effect of noxROS and mtROS seems to result from the frustrated regulation of mtROS by HIF-1 and μ_{34}. Therefore, feedback loops between mtROS, HIF-1, μ_{34}, and μ_{200} together control the appearance of the E/M-W/O state.

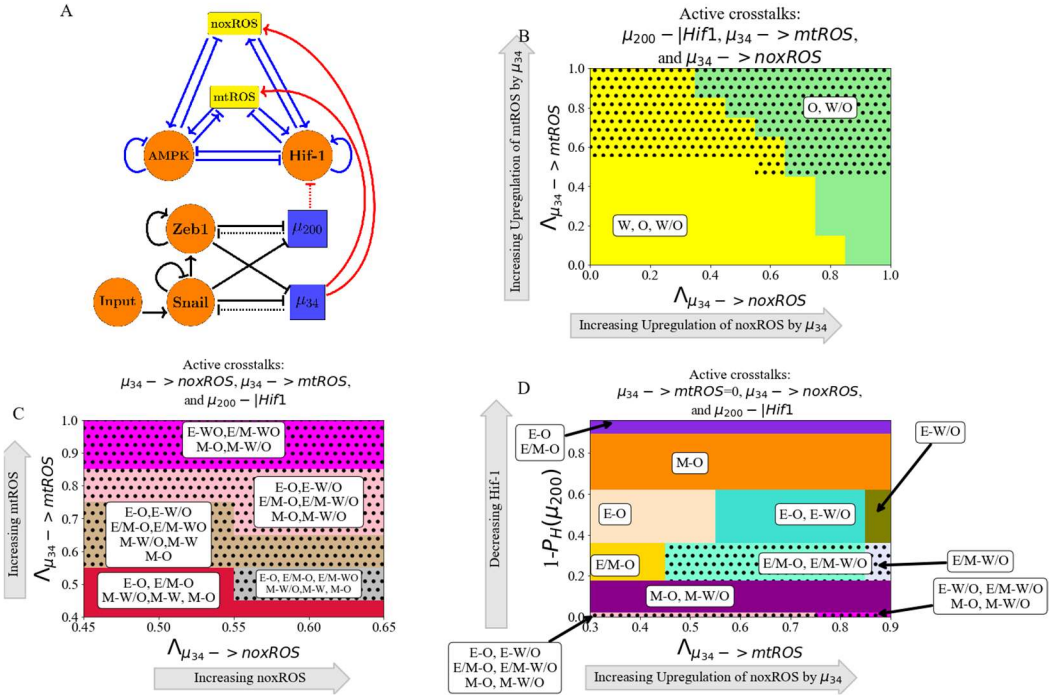

Figure 3. μ_{200} and μ_{34} can upregulate the W/O phenotype. The E/M-W/O state can also be upregulated and mtROS seems to be a key regulator. **(A)** Schematic illustration of the coupled metabolic (top) and EMT (bottom) networks with all miRNA-mediated regulatory links active (μ_{34} upregulating mtROS, μ_{34} upregulating noxROS, and μ_{200} silencing HIF-1). **(B)** The phase plane corresponding to all miRNA-mediated links (pictured in A). In this phase plane, μ_{200} silencing HIF-1 corresponds to the rightmost blue region of Fig. S6 (all metabolic phenotypes are possible), increased noxROS suppresses the W state, and increasing mtROS causes the E/M-W/O coupled state to appear (black dotted region). **(C)** The coupled states of (B), zoomed in on

the middle region. The E/M-W/O state exists when mtROS is upregulated. **(D)** At maximum noxROS levels, increased mtROS levels (x-axis), and moderately silenced HIF-1 (y-axis) there are regions where the E/M-W/O state is possible (black dotted regions).

Metabolic reprogramming can drive EMT: We next consider information flowing in the opposite direction, from metabolism to EMT and determine the effect of each metabolism-driven crosstalk on the coupled states. First, we analyzed the links in which HIF-1 upregulates SNAIL (Fig. 4A and S9) or inhibits μ_{200} (Fig. S10). As expected, both HIF-1 mediated links push the system towards the M state. Further, both the E and E/M states are most associated with the O state (when the HIF-1 level is relatively low) while the M state is initially associated with the W state. This correlation between the E-O and M-W states is assumed in much of the literature [24]. Similarly, modulating the EMT-inducing signals, such as TGF-β, that activate SNAIL can alter the stability of the E/M state and the coupled states (see Fig. S11). Opposite to the HIF1-mediated crosstalks, AMPK-mediated crosstalks (upregulating μ_{200}, downregulating SNAIL, or downregulating ZEB) push the EMT network to adopt an E state and suppress the E/M state, followed by the suppression of the M state (Fig. 4B and S12-S14). Additionally, when AMPK regulates the EMT circuit alone, the E and M states are still most associated with the O and W states, however, the E/M state is associated with the W state. This is in direct contrast to HIF-1 driven crosstalk in which the E/M state is coupled with O state. The results suggest the E/M state has metabolic plasticity because neither OXPHOS nor Warburg metabolism automatically associate with it.

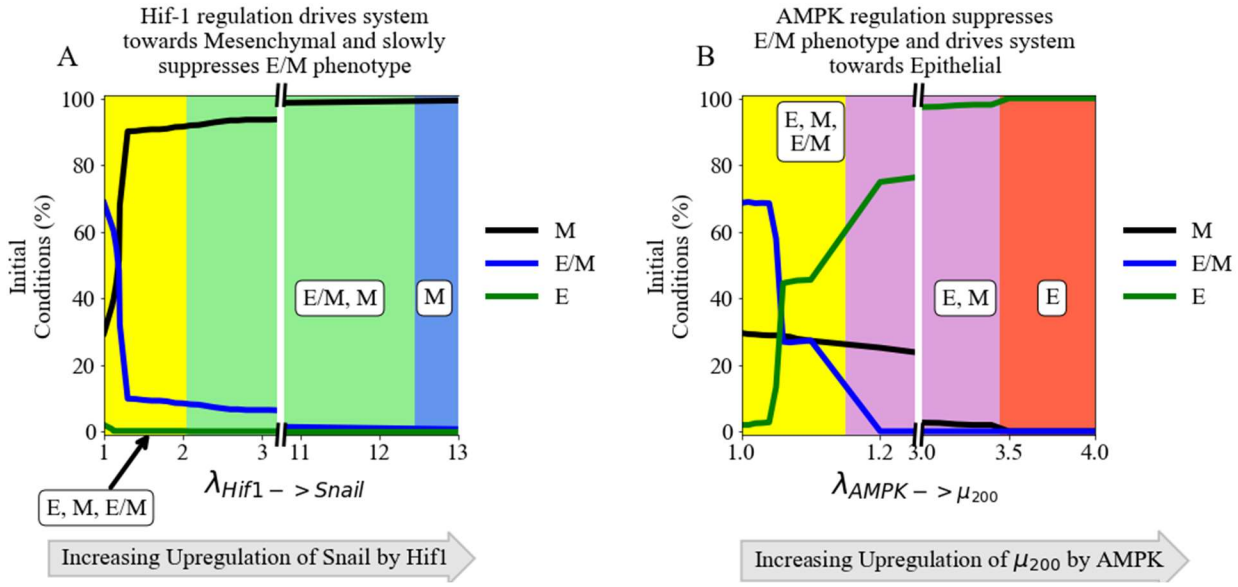

Figure 4. The role of metabolism in driving EMT. HIF-1 mediated crosstalks drive the EMT circuit towards the M state, while AMPK mediated crosstalks drive the EMT network towards the E state. **(A)** The frequency of the E/M, M, or E state as HIF-1 upregulates SNAIL and drives the EMT network towards mesenchymal. **(B)** The frequency of the E/M, M, or E state as AMPK upregulates μ_{200} and drives the system towards epithelial. The E/M state exists for larger portions of the parameter spaces for HIF-1 regulation than for AMPK-mediated crosstalks.

TFs of the metabolic network can stabilize the E/M phenotype: Two distinct events are at play when the metabolic network regulates the EMT circuit. AMPK regulation quickly suppresses the E/M state and pushes the system towards the E state, whereas HIF-1 regulation can allow the system to maintain the E/M state for a range of strengths while ultimately pushing the system towards the M state (Fig. 4A and 4B). Thus, HIF-1 and AMPK-mediated crosstalk should act antagonistically to stabilize the hybrid state.

When at least one of the AMPK crosstalks and one of the HIF-1 crosstalks are activated, the E/M state is stabilized. Additionally, if AMPK and HIF-1 target different EMT-TFs, the E/M-W/O state may exist in larger parameter spaces than if they target the same EMT-TF (Fig.

S15). This suggests activating multiple crosstalks and targeting multiple TFs is likely to stabilize the E/M-W/O state. Therefore, if all HIF-1 and AMPK-mediated crosstalks are active (Fig. 5A) then significant regions occur in which the E/M state exists (Fig. 5B). However, the E/M-W/O state only exists in a small region where μ_{200} is minimally upregulated. Moreover, HIF-1 driven crosstalks can maintain the E/M state longer than AMPK driven crosstalks suggesting, the reduction of the E/M-W/O state is likely due to the suppression of the E/M state by AMPK-mediated crosstalks, as mentioned above (see Fig. S12-S14). This suggests HIF-1 driven crosstalk is more strongly correlated with the E/M state than AMPK driven crosstalk.

If all EMT regulating crosstalks are active, then there are regions where the E/M-W/O state exists. Additionally, the E state is typically coupled to the O state (E-O), the M state is associated with the W state (M-W), and when the E/M state is present it is typically associated with the hybrid W/O state (Fig. 5C). In fact, for any system, if only three coupled states are available and each has a distinct phenotype of the EMT and metabolic networks, then the only possible set of states is E-O, M-W, and E/M-W/O. This behavior represents the full coordination of EMT and metabolism and suggests clusters of migrating cells utilize a combination of aerobic glycolysis and OXPHOS. Given tumors are metabolically heterogeneous, this result suggests the topology and parameters of the system may only represent certain microenvironments and is a limitation of our study.

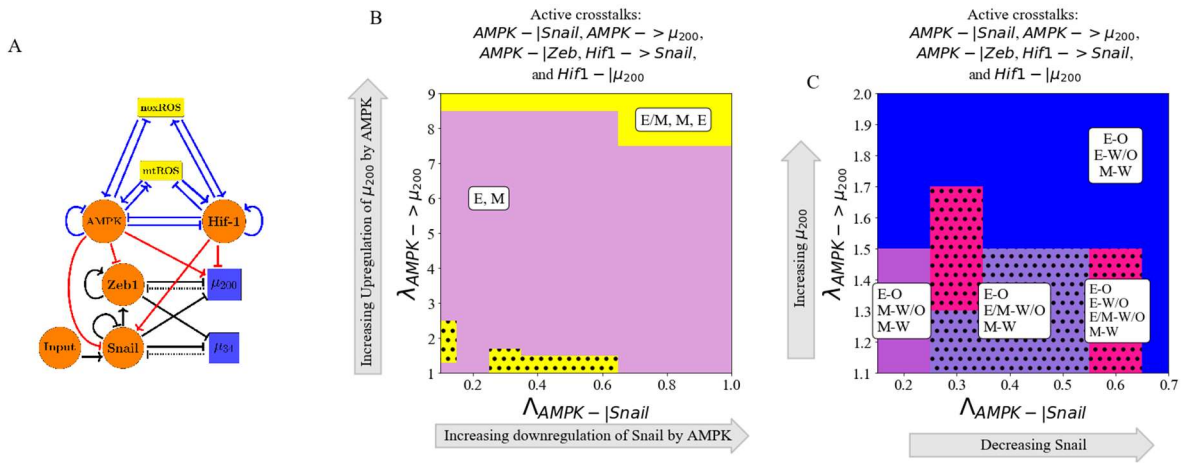

Figure 5. AMPK and HIF-1 cooperate to upregulate the hybrid E/M state. When all HIF-1 and AMPK controlled crosstalks are active (HIF1->Snail, HIF1-|μ_{200}, AMPK-|Snail, AMPK-|Zeb, AMPK-> μ_{200}) the E/M-W/O state can be stabilized. The metabolism-mediated crosstalks work antagonistically to stabilize the E/M state. **(A)** Schematical illustration of the network showing the metabolism-mediated crosstalk. **(B)** The phase plane of potential EMT states when all metabolic driven crosstalks are active. The E/M state is only accessible when $\lambda_{AMPK->\mu200}$ is near 1 or very high (i.e., at the extremes of regulation). **(C)** The coupled states when the EMT circuit is regulated by the metabolic circuit (pictured in A). The results suggest a direct correlation between the E, E/M, and M states to the O, W/O, and W states, respectively.

The Hybrid E/M-W/O phenotype: Recently, it has been suggested the most aggressive cancer phenotype is characterized by the hybrid E/M or W/O states [24]. Therefore, we now focus on how the crosstalk between EMT and metabolism networks affects the E/M-W/O state.

The hybrid E/M-W/O state can be promoted for multiple combinations of crosstalk. For example, the E/M-W/O state can be stabilized when AMPK downregulates SNAIL, HIF-1 downregulates μ_{200}, and μ_{34} upregulates mtROS (Fig. 6A and S16A). Further, the E/M-W/O state become more prevalent when replacing HIF-1 downregulating μ_{200} by increasing the EMT inducing signal to SNAIL (Fig. 6B and S16B). Interestingly, while the E/M-W/O state was stabilized in both cases (Fig. 6A-B), neither set of crosstalk could enable only the E/M-W/O state. However, it is possible to enable only the E/M-W/O state with just three regulatory links;

HIF-1 inhibiting μ_{200}, μ_{34} upregulating mtROS, and modulating the EMT-inducing signal (Fig. 6C and S16C). Additionally, this region, which only includes the E/M-W/O state, persists if all crosstalks are activated (Fig. 6D and S16D).

The proximal phases of the phase enabling only the E/M-W/O state suggests stabilization of the E/M-W/O state requires mutual activation between metabolism and EMT. When the E/M-W/O state is the only available coupled state, the surrounding phases (E-O and E-W/O) are the same whether only three crosstalks (Fig. 6C) or all crosstalks (Fig. 6D) are active, suggesting there may be a sequential path to generate the E/M-W/O state. Further, if the E/M-W/O state is not the only allowed state (Fig. 6A-B), the surrounding phases include both E-associated and M-associated states. Together, the results suggest to reach the E/M-W/O state, epithelial cancer cells first undergo metabolic reprogramming (acquiring the E-W/O state), followed by partial EMT (E/M-W/O). Although it is outside the scope of this manuscript, other crosstalk combinations may also stabilized the E/M-W/O state, and based on these results we would expect HIF-1 suppressing μ_{200} and μ_{34} upregulating mtROS to be prominent among all such combinations.

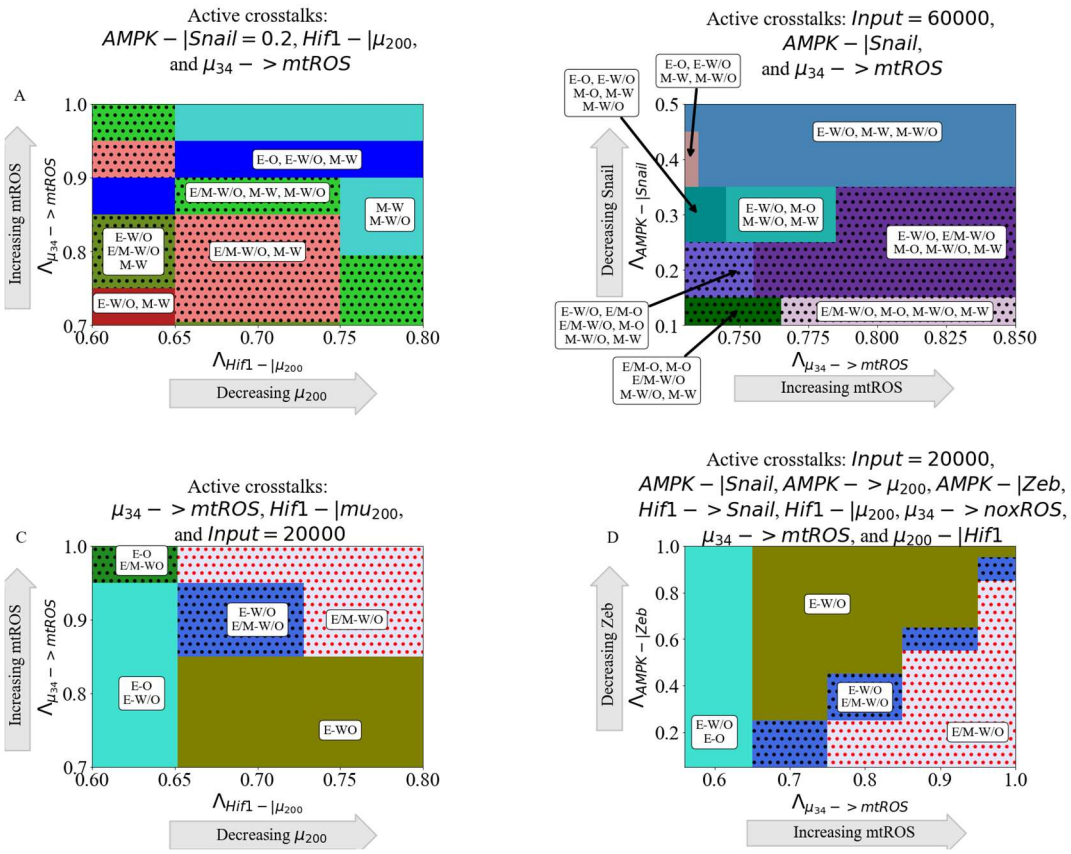

Figure 6. The coupling of the EMT and metabolic regulatory networks can enable a coupled hybrid E/M-W/O state. Minimally, three links (one effecting the metabolic network and two controlling the EMT network) are necessary to enable only the E/M-W/O state. **(A)** Phase diagrams of the coupled states when considering three crosstalks; the Input=60000 molecules, AMPK downregulates SNAIL, and μ_{34} upregulates mtROS. The E/M-W/O state is promoted when mtROS levels are increased. **(B)** The phase diagram of the coupled states when considering AMPK inhibiting SNAIL, HIF-1 inhibiting μ_{200}, and μ_{34} upregulating mtROS. The E/M-W/O state is stabilized for some regions. **(C)** When considering the bi-directional regulation between EMT and metabolism by the three minimally necessary regulatory links (μ_{34} upregulating mtROS, HIF-1 inhibiting μ_{200}, and an EMT-inducing signal on SNAIL) parameter regions exist enabling only the E/M-W/O state. **(D)** When all crosstalks are active there are regions where only the E/M-W/O state exists. Similar sets of phases in (C) and (D) suggest a progression drives the system towards the E/M-W/O state.

Hybrid phenotypes are enabled by crosstalk in cells initially without the E/M or W/O state:

To investigate whether the crosstalk between EMT and metabolism promotes cancer plasticity

(e.g., by acquiring the hybrid states) we simulate scenarios where the individual EMT and

metabolism networks cannot acquire a hybrid state. This scenario corresponds to normal physiological conditions where we expect most cells will be restricted to a binary choice of E versus M and W versus O [36] (see Fig. S17). Then we systematically analyze whether any crosstalk can enable the hybrid state to emerge.

To analyze how the EMT network can drive metabolic reprogramming, we first kept the individual metabolic circuit as a bistable system where only the W and O states are available (i.e., no W/O state). Through gradually activating the miR-34-mediated links, we found the hybrid W/O state emerges and the E/M-W/O state is stabilized when μ_{34} upregulates mtROS (Fig. 7A) but they do not appear when upregulating noxROS or downregulating HIF-1 (Fig. S18). This suggests, noxROS may play a context-dependent role on the coupled state, while mtROS often stabilizes the E/M-W/O state.

Next to see how metabolic reprogramming can possibly drive the hybrid E/M state, we set the EMT network to be bistable (i.e., unable to acquire the E/M state). We find the E/M state can be generate and coupled with the W/O state when HIF-1 inhibits μ_{200} (Fig. 7B) or HIF-1 upregulates SNAIL (Fig. S19). This suggests the master regulator of glycolysis, HIF-1, can drive cells towards the hybrid E/M state. Conversely, an individual AMPK-mediated crosstalk is unable to generate the hybrid E/M state (Fig. S19). Additionally, as with the tristable networks, two competing crosstalks (e.g., AMPK upregulating SNAIL and HIF-1 downregulating μ_{200}) can stabilize the hybrid E/M-W/O (Fig. S20).

When both networks are in the parameter regime where the hybrid state is not available (i.e., neither the E/M or W/O state), the crosstalk can still enable the emergence of these hybrid states. Recall for the coupled tristable circuits, the simplest set of crosstalk with a parameter

region enabling only the E/M-W/O state consisted of three regulatory links; HIF-1 inhibiting μ_{200}, μ_{34} upregulating mtROS, and EMT-inducing signaling acting on SNAIL. When these same links are active for the bistable EMT and metabolism circuits, there are parameter spaces where only the E/M-W/O state are enabled, the results qualitatively agree with the tristable circuit results (Fig. 7C and S21 compared to Fig. 6C).

In summary μ_{34} upregulating mtROS can generate the W/O state and upregulate the E/M-W/O state when the metabolism circuit itself can only acquire the W and O states. Conversely, a HIF-1 mediated crosstalk can generate the E/M state and stabilize the E/M-W/O state even when the EMT circuit itself cannot acquire the E/M state. If both networks are bistable it is possible to enable only the E/M-W/O state with three regulations. These results suggest the E/M-W/O state can be generated and promoted by the crosstalk, independent of the initially available states.

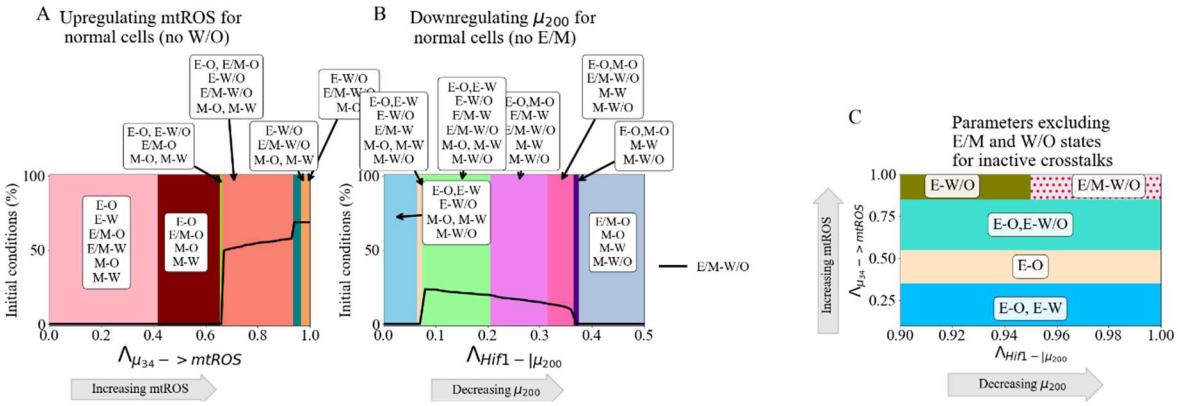

Figure 7. Crosstalk can generate the hybrid states. The activation of a single crosstalk can generate the hybrid state of the downstream network (W/O or E/M). **(A)** The phase diagram showing coupled states for the bistable metabolism network (O or W when the crosstalk is inactive $\lambda_{\mu_{34}->mtROS} = 1.$). Once mtROS is increased (near $\lambda_{\mu 34} = 0.35$), there is a sharp change with the hybrid W/O state becoming the most often occupied state. **(B)** The phase diagram of coupled states when the hybrid E/M state is not available initially when the crosstalk is inactive. As mir200 decreases, the E/M state becomes accessible. **(C)** Combining the models from (A) and (B), we generate a network which only has 4 possible coupled states if the crosstalk is inactive (E-O, E-W, M-O, and M-W). At maximum upregulation of mtROS and downregulation of μ_{200}, only the E/M-W/O state is enabled, similar to Fig. 6C.

GRHL2 and OVOL can stabilize the coupled E/M-W/O state: Previously, we reported transcription factors, such as OVOL and GRHL2 can stabilize the hybrid E/M state [7,37], referred to as the phenotypic stability factors (PSFs) of the E/M state. We are curious how these PSFs regulate the coupling of the E/M state with metabolism states, specifically the E/M-W/O state. We extended the original coupled EMT-metabolism network by including OVOL and GRHL2 (Fig. 8A, parameters and modified equations of the PSF stabilized network are in Section S1.6). When a single crosstalk is active, the E/M-W/O state can exist for the entire parameter space when one of the following crosstalk is active - AMPK downregulating SNAIL, AMPK upregulating μ_{200}, μ_{34} upregulating mtROS, or μ_{34} upregulating noxROS (see Fig. S22). The E/M-W/O state is also stabilized when HIF-1 downregulates μ_{200} or upregulates SNAIL (Fig. S22).

Next, we studied the effect of the PSFs when multiple crosstalks are active. If two competing crosstalks acting on the EMT circuit are active (e.g., one HIF-1 and one AMPK mediated crosstalk), the E/M-W/O state is available for most of the parameter space (Fig. 8B). Further, the E/M-W/O state can be stabilized by activating the three crosstalks (i.e., μ_{34} upregulating mtROS, HIF-1 downregulating μ_{200}, and including the EMT-inducing signaling acting on Snail) that enable only the E/M-W/O state in the absence of these PSFs. Additionally, the parameter space enabling only E/M-W/O is much larger in the presence of the PSFs (Fig. 8C-D and S23) relative to the absence of the PSFs. Further, the coupled states in the phases surrounding the phase containing only the E/M-W/O state are the same as those identified in the absence of PSFs (Fig. 8B). These results show the PSFs can stabilize the coupled E/M-W/O state.

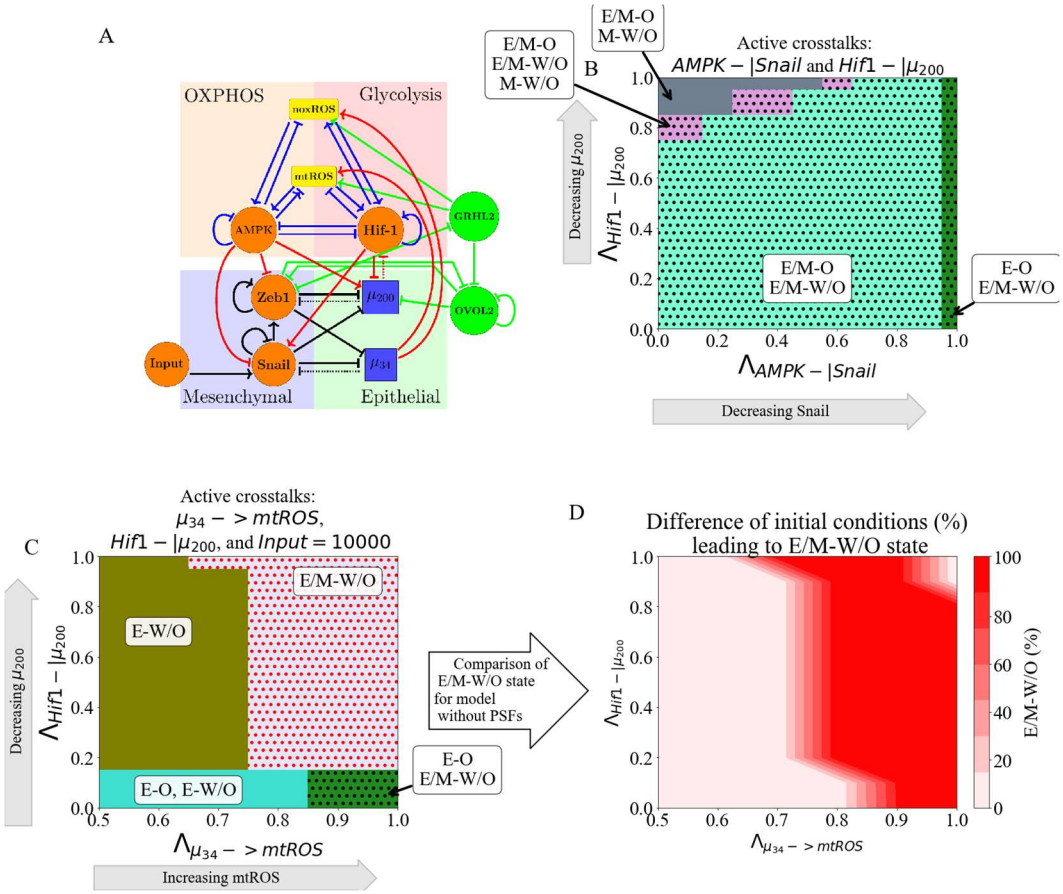

Figure 8. PSFs stabilizing the E/M state can stabilize the association of the E/M state with the W/O state. (A) The coupled EMT-metabolism network including PSFs GRHL2 and OVOL2. **(B)** The phase diagram of the coupled states shows the E/M-W/O state is present in a larger parameter space due to the PSFs stabilizing the E/M state. **(C)** The phase diagram of the coupling states when the three links (μ_{34}-> mtROS, HIF1-$|\mu_{200}$, and reducing the EMT-inducing signal) are active. The parameter regime of the phase enabling only the E/M-W/O state is significantly enlarged compared to the coupled network without PSFs. **(D)** The difference in the frequency of the E/M-W/O state between (C, PSFs present) and the original model (Fig. S23, PSFs not present). The dark red region shows the phases where only the PSF stabilized model can enable the E/M-W/O state, whereas the top right corner is the region where only the E/M-W/O state enabled irrespective of the presence of PSFs.

Discussion

Cancer malignancy relies on the orchestration of multiple hallmarks driven by different functional modules, such as metabolism and stemness [1]. It has become increasingly clear different hallmarks of cancer are extensively coupled. In this work, we focused on how reprogrammed cancer metabolism is coordinated with cancer metastasis. As EMT is often

employed by cancer as part of the metastasic process, we analyzed the mutual regulation between metabolism and EMT through coupling their corresponding gene regulatory circuits. We systematically analyzed the effect of both individual and multiple crosstalks on each of the nine coupled states. The stability of the coupled states was found to vary depending on which crosstalk was active, and multiple crosstalks could exhibit synergistic or antagonistic effects. Therefore, we primarily focused on the E/M-W/O state, as we expect these cells to be the most metastatically capable. We found (1) the E/M-W/O state can be stabilized by a single crosstalk mediated by miR-34 or two antagonistic EMT-driven crosstalks; (2) the similarities between the effects of different crosstalk (e.g., HIF1 suppressing μ_{200} compared to HIF-1 upregulating SNAIL) suggest a degree of consistency in how EMT drives metabolic reprogramming, and vice versa; (3) if crosstalk is bidirectional, it is possible to enable only the E/M-W/O state and this stabilization can be facilitated even under conditions when the individual core circuits do not generate hybrid states; (4) the E/M stabilizing PSFs (OVOL, GRHL2) also stabilize the coupled E/M-W/O state. Together, the results highlight the vital role of the EMT-metabolism crosstalk in mediating cancer metastasis.

The results of our model suggest metabolic reprogramming can drive EMT, but metabolic reprogramming does not have to be complete before EMT begins; this feature allows stabilizing of the most aggressive E/M-W/O state. Further, we identified a scenario wherein the system can follow a progression from the E-O state, first undergoing metabolic reprogramming while maintaining epithelial characteristics (E-W/O state), before undergoing partial EMT to stabilize the E/M-W/O state. Strikingly, the prevalence of the E/M-W/O state is increased by EMT-metabolism crosstalk regardless of initial phenotypic availability (i.e., whether the initial system is significantly E/M-W/O or only E-O, E-W, M-O, and M-W). Therefore, our current

model provides a possible explanation for the mutual activation of metabolic reprogramming and EMT, depending on the initiating signal.

Our findings indicate all else being equal, undergoing EMT tends to correlate with using additional glycolysis. This qualitatively agrees with a recent pan-cancer study based on NCBI GEO microarray datasets and other studies [24,38]. We find HIF-1 (a marker of glycolysis) is strongly associated with EMT, suggesting the E/M state can be stabilized if HIF-1 (glycolysis) is upregulated. Additionally, our model predicts the coupling of the hybrid E/M state and high glycolysis/high OXPHOS (W/O). Notably, our model is unable to explain the cases wherein low glycolysis metabolism is correlated with EMT. However, extending the model to explicitly include coupling with additional metabolic pathways[39] may be able to explain the low glycolysis states of the pan-cancer study [38].

The coupling of the E/M and W/O states is somewhat surprising given the widespread impression that primary tumors often exhibit the Warburg effect, possibly because of their need to limit the amount of ATP produced in favor of maximizing biomass production and growth (see [40] and references therein). However, this finding is consistent with the general idea that moving from E to E/M correlates to increasing stemness, and stem-like capabilities often rely on glycolysis. It is also consistent with HIF-1 activation diminishing OXPHOS while driving EMT. Note this tendency might be over-ridden for cells requiring sufficient energy production to enable motility, such as leader cells. One possibility is during the transition between E-O to E-W/O, when cells first become malignant, the Warburg effect is activated. Then as cells undergo EMT they tend to switch to more W until reaching a mesenchymal-like E/M state with mostly W. Lastly, as cells complete EMT and fully differentiate, they revert back to using mostly OXPHOS. The connection between EMT and metabolism may also depend on other external

signals, such as the level of oxygen in the TME. For example, mesenchymal cells that reduce proliferation and have to traverse the extracellular matrix should switch to more OXPHOS, whereas ones that become quiescent in a hypoxic metastatic niche should favor glycolysis. Resolution of this issue must await a more precise idea of the phrase 'all else being equal'.

The importance of the μ_{34}/μ_{200}/HIF-1/ROS/SNAIL axis for the regulation of the E/M-W/O state arises from our analysis. Our results suggest mtROS is critical for the metabolic activation of EMT, in agreement with recent experimental work that posited mtROS can drive EMT [41], control cancer invasiveness [42], and have a stronger role than noxROS [41,43]. Our results also suggest the mtROS/HIF-1 axis is critical to stabilizing the highly aggressive E/M-W/O state, and this axis has previously been associated with hypoxia-induced cancer aggressiveness [44]. Additionally, both mtROS and HIF-1 are controlled by the miRNAs of the EMT network, μ_{34} and μ_{200}, confirming the importance of miRNAs in mediating the coupling of EMT and metabolism [45]. While we have parametrized the model with values from literature whenever available to ensure biological relevance, one limitation of this study is knowing how these results translate to experimental cancer studies. Thus, the significance of the mtROS/HIF-1 feedback loop should be experimentally tested by e.g., modulating ROS level via antioxidant factors such as NRF2, or modulating hypoxia to perturb HIF-1.

In line with the above, this work is merely a first step, and it is quite likely incorporating additional pathways, especially those regulating cell motility, may be necessary to fully decode EMT-metabolism coupling. For instance, the RHO-ROCK signaling network regulates the transition of cancer cells from collective migration of E/M cells to individual migration of amoeboid cells [13,46]. Inclusion of RHO-ROCK signaling could provide a detailed understanding of how metabolism is coupled to different modes of cancer cell migration.

Overall, the importance of external signaling in our model is in conceptual agreement with a hypothesis by Sciacovelli and Frezza that, in an adverse TME, metabolic reprogramming drives EMT to allow cells to find favorable metabolic niches [28].

The overall goal of this project is toward understanding all the interrelated aspects of cancer metastasis. Previous studies coupling EMT, stemness, and Notch signaling have shown therapy resistance and increased metastatic potential are associated with stem-like hybrid E/M cells [47–49]. Furthermore, these couplings also resulted in unexpected behaviors such as the co-localization of hybrid E/M cells [47] and a tunable stemness window [48]. Studying individual gene regulatory network modules, even in the presence of signals, is unable to give a thorough understanding of the network properties. Therefore, multiple modules and their crosstalk should be studied concurrently to understand the correlation between cancer traits and potentially identify key regulators.

Acknowledgements

This work was supported by National Science Foundation by sponsoring the Center for Theoretical Biological Physics – award PHY-2019745 (JNO, HL) and by awards PHY-1605817 (HL), CHE-1614101 (JNO), and PHY-1522550 (JNO, MG). JNO is a CPRIT Scholar in Cancer Research. MG was also supported by the NSF GRFP no. 1842494.

References

1. Hanahan D. 2022 Hallmarks of Cancer: New Dimensions. *Cancer Discov* 12, 31–46. (doi:10.1158/2159-8290.cd-21-1059)

2. Hay ED. 2005 The mesenchymal cell, its role in the embryo, and the remarkable signaling mechanisms that create it. *Dev Dynam* 233, 706–720. (doi:10.1002/dvdy.20345)

3. Pietilä M, Ivaska J, Mani SA. 2016 Whom to blame for metastasis, the epithelial–mesenchymal transition or the tumor microenvironment? *Cancer Lett* 380, 359–368. (doi:10.1016/j.canlet.2015.12.033)

4. Cho ES, Kang HE, Kim NH, Yook JI. 2019 Therapeutic implications of cancer epithelial-mesenchymal transition (EMT). *Arch Pharm Res* 42, 14–24. (doi:10.1007/s12272-018-01108-7)

5. Fustaino V, Presutti D, Colombo T, Cardinali B, Papoff G, Brandi R, Bertolazzi P, Felici G, Ruberti G. 2017 Characterization of epithelial-mesenchymal transition intermediate/hybrid phenotypes associated to resistance to EGFR inhibitors in non-small cell lung cancer cell lines. *Oncotarget* 8, 103340–103363. (doi:10.18632/oncotarget.21132)

6. George JT, Jolly MK, Xu J, Somarelli J, Levine H. 2017 Survival outcomes in cancer patients predicted by a partial EMT gene expression scoring metric. *Cancer Res* 77, canres.3521.2016. (doi:10.1158/0008-5472.can-16-3521)

7. Jolly MK *et al.* 2016 Stability of the hybrid epithelial/mesenchymal phenotype. *Oncotarget* 7, 27067–27084. (doi:10.18632/oncotarget.8166)

8. Pastushenko I *et al.* 2018 Identification of the tumour transition states occurring during EMT. *Nature* 556, 463–468. (doi:10.1038/s41586-018-0040-3)

9. Simeonov KP, Byrns CN, Clark ML, Norgard RJ, Martin B, Stanger BZ, Shendure J, McKenna A, Lengner CJ. 2021 Single-cell lineage tracing of metastatic cancer reveals selection of hybrid EMT states. *Cancer Cell* 39, 1150-1162.e9. (doi:10.1016/j.ccell.2021.05.005)

10. Lu M, Jolly MK, Levine H, Onuchic JN, Ben-Jacob E. 2013 MicroRNA-based regulation of epithelial–hybrid–mesenchymal fate determination. *Proc National Acad Sci* 110, 18144–18149. (doi:10.1073/pnas.1318192110)

11. Saitoh M. 2018 Involvement of partial EMT in cancer progression. *J Biochem* 164, 257–264. (doi:10.1093/jb/mvy047)

12. Bakir B, Chiarella AM, Pitarresi JR, Rustgi AK. 2020 EMT, MET, Plasticity, and Tumor Metastasis. *Trends Cell Biol* 30, 764–776. (doi:10.1016/j.tcb.2020.07.003)

13. Saxena K, Jolly MK, Balamurugan K. 2020 Hypoxia, partial EMT and collective migration: Emerging culprits in metastasis. *Transl Oncol* 13, 100845. (doi:10.1016/j.tranon.2020.100845)

14. Dey P, Kimmelman AC, DePinho RA. 2021 Metabolic Codependencies in the Tumor Microenvironment. *Cancer Discov* , candisc.1211.2020. (doi:10.1158/2159-8290.cd-20-1211)

15. Warburg O, Wind F, Negelein E. 1927 THE METABOLISM OF TUMORS IN THE BODY. *J Gen Physiol* 8, 519–530. (doi:10.1085/jgp.8.6.519)

16. Liberti MV, Locasale JW. 2016 The Warburg Effect: How Does it Benefit Cancer Cells? *Trends Biochem Sci* 41, 211–218. (doi:10.1016/j.tibs.2015.12.001)

17. Ohshima K, Morii E. 2021 Metabolic Reprogramming of Cancer Cells during Tumor Progression and Metastasis. *Metabolites* 11, 28. (doi:10.3390/metabo11010028)

18. Nagao A, Kobayashi M, Koyasu S, Chow CCT, Harada H. 2019 HIF-1-Dependent Reprogramming of Glucose Metabolic Pathway of Cancer Cells and Its Therapeutic Significance. *Int J Mol Sci* 20, 238. (doi:10.3390/ijms20020238)

19. Cheng Y *et al.* 2018 Metastatic cancer cells compensate for low energy supplies in hostile microenvironments with bioenergetic adaptation and metabolic reprogramming. *Int J Oncol* 53, 2590–2604. (doi:10.3892/ijo.2018.4582)

20. Yu L, Lu M, Jia D, Ma J, Ben-Jacob E, Levine H, Kaipparettu BA, Onuchic JN. 2017 Modeling the Genetic Regulation of Cancer Metabolism: Interplay between Glycolysis and Oxidative Phosphorylation. *Cancer Res* 77, 1564–1574. (doi:10.1158/0008-5472.can-16-2074)

21. Porporato PE *et al.* 2014 A Mitochondrial Switch Promotes Tumor Metastasis. *Cell Reports* 8, 754–766. (doi:10.1016/j.celrep.2014.06.043)

22. Jia D, Park JH, Jung KH, Levine H, Kaipparettu BA. 2018 Elucidating the Metabolic Plasticity of Cancer: Mitochondrial Reprogramming and Hybrid Metabolic States. *Cells* 7, 21. (doi:10.3390/cells7030021)

23. Dupuy F *et al.* 2015 PDK1-Dependent Metabolic Reprogramming Dictates Metastatic Potential in Breast Cancer. *Cell Metab* 22, 577–589. (doi:10.1016/j.cmet.2015.08.007)

24. Jia D *et al.* 2021 Towards decoding the coupled decision-making of metabolism and epithelial-to-mesenchymal transition in cancer. *Brit J Cancer* , 1–10. (doi:10.1038/s41416-021-01385-y)

25. Sung J-Y, Cheong J-H. 2021 Pan-Cancer Analysis Reveals Distinct Metabolic Reprogramming in Different Epithelial–Mesenchymal Transition Activity States. *Cancers* 13, 1778. (doi:10.3390/cancers13081778)

26. Choudhary KS, Rohatgi N, Halldorsson S, Briem E, Gudjonsson T, Gudmundsson S, Rolfsson O. 2016 EGFR Signal-Network Reconstruction Demonstrates Metabolic Crosstalk in EMT. *Plos Comput Biol* 12, e1004924. (doi:10.1371/journal.pcbi.1004924)

27. Feng S, Zhang L, Liu X, Li G, Zhang B, Wang Z, Zhang H, Ma H. 2020 Low levels of AMPK promote epithelial-mesenchymal transition in lung cancer primarily through HDAC4-

and HDAC5-mediated metabolic reprogramming. *J Cell Mol Med* 24, 7789–7801. (doi:10.1111/jcmm.15410)

28. Sciacovelli M, Frezza C. 2017 Metabolic reprogramming and epithelial-to-mesenchymal transition in cancer. *Febs J* 284, 3132–3144. (doi:10.1111/febs.14090)

29. Huang R, Zong X. 2017 Aberrant cancer metabolism in epithelial–mesenchymal transition and cancer metastasis: Mechanisms in cancer progression. *Crit Rev Oncol Hemat* 115, 13–22. (doi:10.1016/j.critrevonc.2017.04.005)

30. Kang X, Wang J, Li C. 2019 Exposing the Underlying Relationship of Cancer Metastasis to Metabolism and Epithelial-Mesenchymal Transitions. *Iscience* 21, 754–772. (doi:10.1016/j.isci.2019.10.060)

31. LeBleu VS *et al.* 2014 PGC-1α mediates mitochondrial biogenesis and oxidative phosphorylation in cancer cells to promote metastasis. *Nat Cell Biol* 16, 992–1003. (doi:10.1038/ncb3039)

32. Bocci F *et al.* 2019 NRF2 activates a partial epithelial-mesenchymal transition and is maximally present in a hybrid epithelial/mesenchymal phenotype. *Integr Biol* 11, 251–263. (doi:10.1093/intbio/zyz021)

33. Luo M *et al.* 2018 Targeting Breast Cancer Stem Cell State Equilibrium through Modulation of Redox Signaling. *Cell Metab* 28, 69-86.e6. (doi:10.1016/j.cmet.2018.06.006)

34. Colacino JA *et al.* 2018 Heterogeneity of Human Breast Stem and Progenitor Cells as Revealed by Transcriptional Profiling. *Stem Cell Rep* 10, 1596–1609. (doi:10.1016/j.stemcr.2018.03.001)

35. Lu M, Jolly MK, Gomoto R, Huang B, Onuchic J, Ben-Jacob E. 2013 Tristability in Cancer-Associated MicroRNA-TF Chimera Toggle Switch. *J Phys Chem B* 117, 13164–13174. (doi:10.1021/jp403156m)

36. Tripathi S, Kessler DA, Levine H. 2020 Biological Networks Regulating Cell Fate Choice Are Minimally Frustrated. *Phys Rev Lett* 125, 088101. (doi:10.1103/physrevlett.125.088101)

37. Jia D, Li X, Bocci F, Tripathi S, Deng Y, Jolly MK, Onuchic JN, Levine H. 2019 Quantifying Cancer Epithelial-Mesenchymal Plasticity and its Association with Stemness and Immune Response. *J Clin Medicine* 8, 725. (doi:10.3390/jcm8050725)

38. Muralidharan S, Sahoo S, Saha A, Chandran S, Majumdar SS, Mandal S, Levine H, Jolly MK. 2022 Quantifying the Patterns of Metabolic Plasticity and Heterogeneity along the Epithelial–Hybrid–Mesenchymal Spectrum in Cancer. *Biomol* 12, 297. (doi:10.3390/biom12020297)

39. Jia D, Lu M, Jung KH, Park JH, Yu L, Onuchic JN, Kaipparettu BA, Levine H. 2019 Elucidating cancer metabolic plasticity by coupling gene regulation with metabolic pathways. *Proc National Acad Sci* 116, 201816391. (doi:10.1073/pnas.1816391116)

40. Tripathi S, Park JH, Pudakalakatti S, Bhattacharya PK, Kaipparettu BA, Levine H. 2022 A mechanistic modeling framework reveals the key principles underlying tumor metabolism. *Plos Comput Biol* 18, e1009841. (doi:10.1371/journal.pcbi.1009841)

41. Radisky DC *et al.* 2005 Rac1b and reactive oxygen species mediate MMP-3-induced EMT and genomic instability. *Nature* 436, 123–127. (doi:10.1038/nature03688)

42. Ishikawa K, Takenaga K, Akimoto M, Koshikawa N, Yamaguchi A, Imanishi H, Nakada K, Honma Y, Hayashi J-I. 2008 ROS-Generating Mitochondrial DNA Mutations Can Regulate Tumor Cell Metastasis. *Science* 320, 661–664. (doi:10.1126/science.1156906)

43. Kovac S, Angelova PR, Holmström KM, Zhang Y, Dinkova-Kostova AT, Abramov AY. 2015 Nrf2 regulates ROS production by mitochondria and NADPH oxidase. *Biochimica Et Biophysica Acta Bba - Gen Subj* 1850, 794–801. (doi:10.1016/j.bbagen.2014.11.021)

44. SHIDA M, KITAJIMA Y, NAKAMURA J, YANAGIHARA K, BABA K, WAKIYAMA K, NOSHIRO H. 2016 Impaired mitophagy activates mtROS/HIF-1α interplay and increases cancer aggressiveness in gastric cancer cells under hypoxia. *Int J Oncol* 48, 1379–1390. (doi:10.3892/ijo.2016.3359)

45. Babaei G, Raei N, milani AT, Aziz SG-G, Pourjabbar N, Geravand F. 2021 The emerging role of miR-200 family in metastasis: focus on EMT, CSCs, angiogenesis, and anoikis. *Mol Biol Rep* 48, 6935–6947. (doi:10.1007/s11033-021-06666-6)

46. Graziani V, Rodriguez-Hernandez I, Maiques O, Sanz-Moreno V. 2021 The amoeboid state as part of the epithelial-to-mesenchymal transition programme. *Trends Cell Biol* 32, 228–242. (doi:10.1016/j.tcb.2021.10.004)

47. Bocci F, Gearhart-Serna L, Boareto M, Ribeiro M, Ben-Jacob E, Devi GR, Levine H, Onuchic JN, Jolly MK. 2018 Toward understanding cancer stem cell heterogeneity in the tumor microenvironment. *Proc National Acad Sci* 116, 201815345. (doi:10.1073/pnas.1815345116)

48. Jolly MK, Jia D, Boareto M, Mani SA, Pienta KJ, Ben-Jacob E, Levine H. 2015 Coupling the modules of EMT and stemness: A tunable 'stemness window' model. *Oncotarget* 6, 25161–25174. (doi:10.18632/oncotarget.4629)

49. Bocci F, Jolly MK, George JT, Levine H, Onuchic JN. 2018 A mechanism-based computational model to capture the interconnections among epithelial-mesenchymal transition, cancer stem cells and Notch-Jagged signaling. *Oncotarget* 9, 29906–29920. (doi:10.18632/oncotarget.25692)